Experimental Ion Mobilities in Liquid He^3 below 1°K*

A. C. ANDERSON, M. KUCHNIR,† AND J. C. WHEATLEY‡
Department of Physics and Materials Research Laboratory, University of Illinois, Urbana, Illinois
(Received 30 November 1967)

The low-field mobility of positive and negative ions in liquid He^3 was measured using a time-of-flight technique for temperatures between 0.03 and 1°K and pressures of 27.9, 7.5, and less than 0.35 atm. Details of the experimental procedures as well as of the experimental apparatus and its construction are presented. The positive-ion mobility μ_+ was found to be larger than the negative μ_-, except at 27.9 atm above 0.3°K, where both are $\sim$0.036 cm²/V sec. By increasing the pressure, μ_- was observed to increase while μ_+ decreased. Furthermore, μ_- was found to be a continuous function of the temperature, reproducible within 1% throughout the entire temperature range of the measurements, whereas μ_+ presented hysteresis in a temperature range that was dependent on the pressure. Some typical mobility values are:

Pressure (atm)	Temp (°K)	μ_+ (cm²/V sec)	μ_- (cm²/V sec)
0.32	0.03	0.160	0.011
	0.30	0.064	0.017
	1.00	0.068	0.028
7.5	0.03	0.140	0.019
	0.30	0.046	0.026
	1.00	0.056	0.038
27.9	0.03	...	0.025
	0.30	0.036	0.033
	1.00	0.037	0.038

The systematic error involved in the absolute value of the mobility is less than 10%. No theoretical calculation presently available correctly predicts μ_- or μ_+.

I. INTRODUCTION

IONS have been used as microscopic probes to obtain information on the nature of the superfluid state of liquid He^4. Their behavior in this liquid can be explained in part as due to scattering by rotons and phonons.[1] Their entrapment by vortex lines and vortex rings[2] has added to our knowledge of these types of collective excitations. It would be interesting to use ions also in liquid He^3 at very low temperatures in order to investigate their behavior in a Fermi fluid. Previous measurements of ion mobility in liquid He^3 by Meyer *et al.*,[3] Modena *et al.*,[4] and Shalnikov[5] did not reach temperatures low enough for the effect of degeneracy in the liquid to appear. We present here data on the mobility as a function of temperature down to 0.03°K at three different pressures: 27.9, 7.5, and less than 0.35 atm. These data provide an experimental basis for theories involving the nature of the ions and their interaction with liquid He^3.

A structure is created around each ion in liquid He because of the high density of the medium and the large local electric field which polarizes the neighboring He atoms. It seems fairly reasonable to assume that the same types of ionic structures are found in both liquid He^3 and liquid He^4. The arguments in favor of this assumption are the chemical similarity of the two isotopes as well as some experimentally observed properties of the ion mobility in the two liquids. For example, in either liquid the positive-ion mobility is larger than the negative-ion mobility and decreases with pressure, while at low pressures the negative-ion mobility increases with pressure.

The model for the positive-ion structure in liquid He^4 has been developed by Atkins.[6,7] It is assumed to be a solid He core created by a localized point charge causing electrostriction in the polarizable liquid around it. The model for the negative-ion structure at low pressures is an electron inside a bubble created in the liquid by the large zero-point energy of the electron. This model, first suggested by Ferrell[8] in order to explain the anomalously long lifetime of a positron in liquid He, has been in-

* Supported in part by the U. S. Atomic Energy Commission under Contract No. AT(11-1)-1198. This work was submitted by M. Kuchnir in partial fulfillment of the requirements for the Ph.D. degree at the University of Illinois.

† Present address: Argonne National Laboratory, Argonne, Ill.

‡ Present address: University of California, San Diego, La Jolla, Calif.

[1] F. Reif and L. Meyer, Phys. Rev. **119**, 1164 (1960).

[2] G. Careri, W. D. McCormick, and F. Scaramuzzi, Phys. Letters **1**, 61 (1962); G. W. Rayfield and F. Reif, Phys. Rev. **136**, A1194 (1964).

[3] L. Meyer, H. T. Davis, S. A. Rice, and R. J. Donnelly, Phys. Rev. **126**, 1927 (1962).

[4] I. Modena, in *Proceedings of the Eighth International Conference on Low Temperature Physics* (Butterworths Scientific Publications, Ltd., London, 1963), p. 51; P. de Magistris and I. Modena, Report No. LNF 63/83, Laboratori Nazionali di Frascati, Rome, 1963 (unpublished); P. de Magistris, I. Modena, and F. Scaramuzzi, in *Low Temperature Physics*, edited by J. G. Daunt *et al.* (Plenum Press, Inc., New York, 1965), Vol. 9, p. 349.

[5] A. I. Shalnikov, Zh. Eksperim. i Teor. Fiz. **41**, 1059 (1961) [English transl.: Soviet Phys.—JETP **14**, 755 (1962)].

[6] K. R. Atkins, Phys. Rev. **116**, 1339 (1959).

[7] K. R. Atkins, in *Proceedings of the Enrico Fermi International School of Physics, Course XXI*, edited by G. Careri (Academic Press Inc., New York, 1963), p. 403.

[8] R. A. Ferrell, Phys. Rev. **108**, 167 (1957).

tensively studied both experimentally[9–12] and theoretically.[13–20] With these models one would expect that an increase in pressure would decrease the radius of the negative-ion structure and increase the radius of the positive-ion structure. The observed pressure dependence of the mobility is directly connected with this dependence of the size of the ion on pressure because, on the basis of qualitative reasoning, one expects the mobility to increase as the ion radius decreases. In liquid He^4 at higher pressures the negative-ion mobility reaches a maximum and again decreases with increasing pressure.[21] This has been interpreted as reflecting the onset of solidification around the bubble.

Besides the dependence on the structure of the ion, the mobility also depends on the nature of the scattering by the liquid. Most experimental transport properties of liquid He^3 can be explained in terms of the Landau-Fermi liquid theory, in which the liquid is assumed to be comprised of quasiparticle fermions interacting strongly with one another.[22,23] At 0.03°K the fermion system is certainly strongly degenerate. One would hope that this fact would simplify the interpretation of our mobility measurements. At very low temperatures, for example, collisions are inhibited by the exclusion principle and the mobility should vary as T^{-2}.[24,25] However, no T^{-2} dependence was observed in our measurements, which extended down to 0.03°K. No existing theoretical calculation gives a complete account of the mobilities, although the pressure dependence and temperature independence of the negative ion mobility below ~0.1°K are in qualitative agreement with the theory of Davis and Dagonnier.[26] At higher temperatures, however, this theory predicts a decrease, rather than an increase, in the mobility.

II. EXPERIMENT

A. Apparatus

Two main techniques were involved in the present work: one to cool the He^3 below 0.3°K and measure its temperature, the other to produce ions in the He^3 and measure their mobility.

The helium cryostat used in this experiment has previously been described by Abel *et al.*[22] In the present experiment, 180 g of CrK alum crystals were used to refrigerate the He^3 and 65 g of Fe alum crystals were used for the thermal guard. For the magnetic cooling a single superconducting[27] solenoid was used. In order to pressurize the He^3 in the cell, the stainless-steel Toepler pump system described by Salinger[28] and by Anderson *et al.*[29] was used with the modifications described by Connolly.[30] The He^4 content of our He^3 sample was measured with a modified Veeco MS9/A leak detector[22] and was found to be less than 130 ppm.

The method used to measure the mobility of the ions is the same as that used by Meyer and Reif,[1] but with appropriate additional modifications for lower temperatures and lower frequencies. The electrode assembly used in the present work is shown schematically in the lower part of Fig. 1. This assembly is located inside an epoxy case, or cell, filled with liquid He^3. The radioactive source S ionizes the He^3 atoms in its immediate vicinity. The voltages supplied to the electrodes produce electric fields that select and drive the ions to the collector C which is connected to an electrometer. A square-wave voltage of frequency ν is simultaneously applied to grids A′ and B′ in order to reverse the field between the pairs

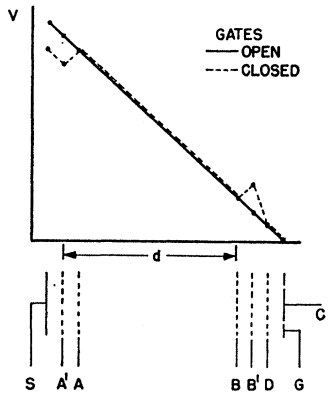

FIG. 1. Voltage distribution and schematic diagram of electrode assembly. Ions produced near the source S drift under the influence of the electric field toward the collector C connected to the electrometer. A square-wave potential is applied to the pairs of grids, A′A and BB′, which act as synchronized gates. D shields C from the square wave, and G guards C from stray surface currents.

[9] W. T. Sommer, Phys. Rev. Letters **12**, 271 (1964).
[10] M. A. Woolf and G. W. Rayfield, Phys. Rev. Letters **15**, 235 (1965).
[11] J. Levine and T. M. Sanders, Jr., Phys. Rev. Letters, **8**, 159 (1962).
[12] B. E. Springett, Phys. Rev. **155**, 139 (1967).
[13] B. Burdick, Phys. Rev. Letters **14**, 11 (1965).
[14] J. Jortner, N. R. Kestner, S. A. Rice, and M. H. Cohen, J. Chem. Phys. **43**, 2614 (1965).
[15] C. G. Kuper, Phys. Rev. **122**, 1007 (1961).
[16] C. G. Kuper, in *Proceedings of the Enrico Fermi International School of Physics, Course XXI*, edited by G. Careri (Academic Press Inc., New York, 1963), p. 414.
[17] K. Hiroike, N. R. Kestner, S. A. Rice, and J. Jortner, J. Chem. Phys. **43**, 2625 (1965).
[18] R. C. Clark, Phys. Letters **16**, 42 (1965).
[19] P. E. Parks and R. J. Donnelly, Phys. Rev. Letters **16**, 45 (1966).
[20] B. E. Springett, M. H. Cohen, and J. Jortner, Phys. Rev. **159**, 183 (1967).
[21] L. Meyer and F. Reif, Phys. Rev. **123**, 727 (1961).
[22] W. R. Abel, W. C. Black, A. C. Anderson, and J. C. Wheatley, Physics **1**, 337 (1965).
[23] W. R. Abel, R. T. Johnson, J. C. Wheatley, and W. Zimmerman, Jr., Phys. Rev. Letters **18**, 737 (1967).
[24] R. Abe and K. Aizu, Phys. Rev. **123**, 10 (1961).
[25] R. C. Clark, Proc. Phys. Soc. (London) **82**, 785 (1963).
[26] H. T. Davis and R. Dagonnier, J. Chem. Phys. **44**, 4030 (1966).
[27] Magnion, Inc., 144 Middlesex Turnpike, Burlington, Mass.
[28] G. L. Salinger, Ph.D. thesis, University of Illinois, 1961 (unpublished).
[29] A. C. Anderson, G. L. Salinger, W. A. Steyert, and J. C. Wheatley, Phys. Rev. Letters, **7**, 295 (1961).
[30] J. I. Connolly, Ph.D. thesis, University of Illinois, 1965 (unpublished).

of grids A′A and BB′ during a half-period. As a result the current i to C is a maximum essentially whenever t, the time required for the ions to drift the distance d from A′ to B under the influence of an electric field $\mathbf{E}$, is equal to an integral number of periods ν^{-1} of the square-wave voltage. Grid D electrostatically shields the sensitive collector C from the square wave at B′, and the guard G prevents stray surface currents from reaching C. The upper half of Fig. 1 indicates the potential distribution when the gates formed by grids A′A and BB′ are open (solid line) and closed (dashed line).

Assume the cell to be free of ions between A′ and C at time $t=0$, when the gates are just opening. Ions start drifting into this region through grid A′ until time $t=(2\nu)^{-1}$ when the fields inside the gates are reversed and hence closed. A bunch of ions is then left drifting in the space AB while the ions caught inside the gate are collected at A′. Since the separation d_A between A and A′ is approximately 11 times shorter than d, the gates will be essentially empty of ions at the time of the next opening of the gates. A maximum part of the bunch will pass the second gate if the front of the bunch reaches B exactly at time $t=n\nu^{-1}$ (where n is an integer) when the gates are opening; otherwise its head, or its tail, will be caught by a closed gate and collected at B. Therefore maxima of i occur for $\nu=\nu_n$ such that

$$d=\int_0^{n\nu_n^{-1}} v\,dt, \tag{1}$$

where $\mathbf{v}=\mu\mathbf{E}$ is the drift velocity of the ions. For a field-independent mobility we can write

$$\mu=\frac{d^2}{|V_{A'}-V_B|}\frac{\nu_n}{n}. \tag{2}$$

This proportionality of ν_n/n to $|V_{A'}-V_B|$ was verified for fields of 24, 60, 68, 89, 136, and 203 V/cm, which permits us to neglect any nonuniformity of the electric field. The values to be used for the distances d, d_A, and d_B (separation between grids B and B′) are not the geometric separation between grids as measured at room temperature but rather an effective separation that compensates for (1) field penetration when the electric field inside the gate is not exactly equal and opposite to the field outside, (2) the thermal contraction of the cell, (3) the nonplanar geometry of the grids, and (4) the straggling of the ions in the extremities of the bunch.

The current $i=i(\nu)$ detected at the collector will be a series of triangular peaks whose symmetry depends on the thicknesses d_A and d_B of the gates. With the assumption that no charge is collected at the walls, it can be shown that the maxima of i occur for ν between

$$\nu=\frac{n\mu}{(d-d_A)^2/|V_A-V_B|+d_A^2/|V_A-V_{A'}|}$$

and

$$\nu=\frac{n\mu}{(d-d_A)^2/|V_A-V_B|+d_B^2/|V_B-V_{B'}|}.$$

The maximum value of the current is

$$i_{\max}=i_0\left\{\frac{1}{2}-nd_A\Big/\left[(d-d_A)\left(\frac{V_{A'}-V_A}{d_A}\frac{d-d_A}{V_A-V_B}\right)+d_A\right]\right\},$$

where i_0 is the current with open gates. For small d_A and d_B, and uniform field throughout the cell, these expressions simplify to $\nu=n\mu(V_{A'}-V_B)/d^2$ and $i_{\max}=i_0(\frac{1}{2}-nd_A/d)$. An actual plot of the current i at the collector as a function of ν is shown in Fig. 2. The nth peak corresponds to the situation in which n small bunches of ions are chopped by a frequency ν_n and travel the distance d during n periods of ν_n^{-1}.

The electronics used in this experiment are schematically shown in Fig. 3. Radio "B" batteries were used to supply the proper voltages to the cell electrodes. The variable resistors shown were used for compensating the voltage drift of the batteries. The gating action was provided by driving a mercury relay with a bistable multivibrator which was triggered by pulses generated by a Tektronics Type 162 waveform generator. These pulses also triggered a Tektronics Type 551 or 531 oscilloscope. The time interval between pulses was measured by an Anadex Model CF-200R Counter.[31] Since the frequencies to be used were low (1–50 Hz) the Anadex Counter actually counted the number of cycles p, generated by its internal 100-kHz crystal oscillator,

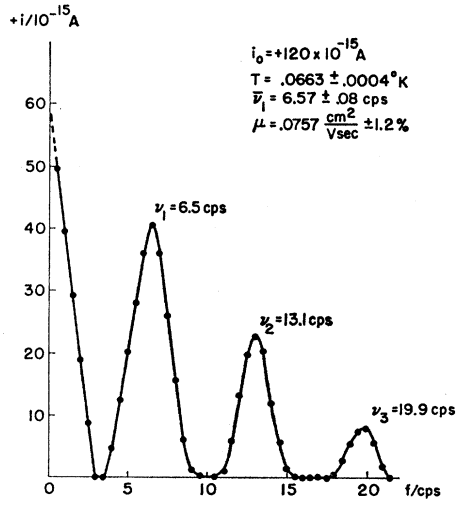

FIG. 2. Ion current i as a function of gate frequency ν.

[31] Anadex Instruments, Inc., 7617 Hayvenhurst Ave., Van Nuys, Calif.

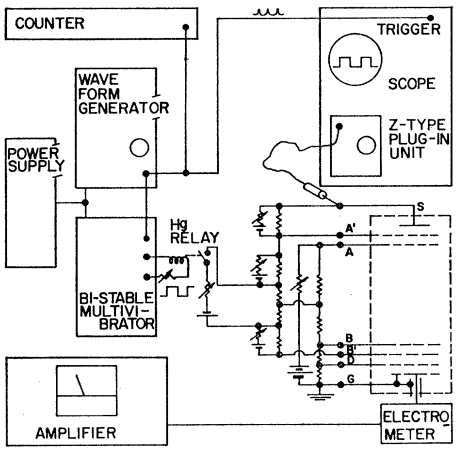

FIG. 3. Schematic diagram of the electronics.

which occurred between two successive trigger pulses. Hence, $\nu = 50\,000/p$ Hz.

The voltage measurements were made rapidly using the oscilloscope with a type Z plug-in unit. This unit is a calibrated differential comparator preamplifier, with a ± 2000-cm dynamic scale length and a large input impedance. In order to reverse the field and measure the mobility of ions of opposite sign, all five batteries had to have their connecting leads reversed. A switch, not shown in Fig. 3, was introduced for this operation and to disconnect the batteries when not in use. A commercially available tritiated titanium foil with a nominal activity of 6.2 mCi/cm^2 was used.[32] A heat leak of less than 50 erg/min and ion currents ranging from 10^{-15} to 10^{-13} A were produced by a disk-shaped source of 0.5 cm diam. The current reaching the collector was detected by a Cary Model 31 Vibrating Reed Electrometer and Amplifier[33] coupled directly through a specially built, rigid coaxial cable.[34]

Figure 4 is a simplified drawing of the cell. For reasons that will be given in Sec. II B, two cells were made. Throughout this work they are referred to as the first and second cells. To thermally connect the He^3 in the cell with the refrigerator, a brush of approximately 9000 copper wires (0.005 cm diam; Heavy Formex Insulated) was made and positioned behind the source. Both cells used the same source and the same brush, and had roughly the same design and dimensions. The magnetic thermometer was located behind the collector. It consisted of a cylindrical space with length and diameter equal to 1.5 cm which was filled with powdered cerium magnesium nitrate (CMN) crystals (3.24 g which passed a NBS No. 40 sieve for the first cell and 3.70 g which passed a NBS No. 60 sieve for the second cell).[35] Pieces of cotton cloth behind the collector and in front of the 0.04-cm o.d. CuNi filling tube kept the powder in place. In order to decrease the thermal resistance between the thermometer and the mobility measuring region the apertures around and behind the collector were designed to provide a maximum area-to-length ratio. The material used in the construction of the case, plug, rings, and brush was Epibond 100 A.[36]

The grids were cut from electroformed gold mesh foils[37] with 40 lines/cm and 82% transparency. To avoid bowing due to thermal contraction, the grids were glued to the rings of the cell at only one spot with silver paint.[38] The collector was a 0.5-cm-diam disk cut from a 0.013-cm-thick gold foil. The collector lead was the inner conductor of the coaxial line leading to the input of the electrometer. Special care was taken to keep this lead very well insulated electrically.

The main difference between the two cells was concerned with the wall of the drift space, which, for the most part, was made electrically conducting to avoid charge buildup. This inner wall was a composite formed by the inner cylindrical surfaces of a stack of rings which were electrically insulated from one another. In the first cell the inner cylindrical surfaces of the rings were painted with electrically conducting silver paint. These cylindrical painted surfaces were separated by electrically insulating grooves. On the short rings, between electrodes that were close together, the painted surfaces were in electrical contact with the adjacent electrodes.

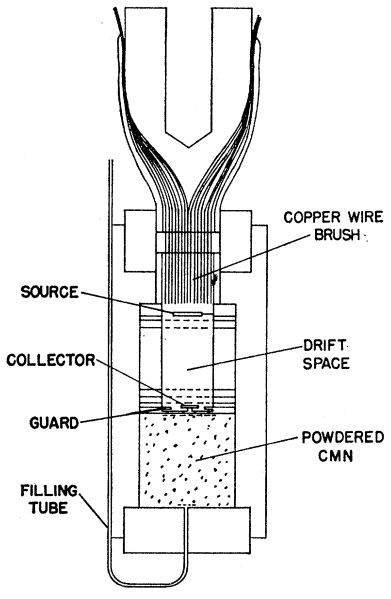

FIG. 4. Schematic diagram of the mobility cell. The volume of liquid He^3 in the cell was ~ 2.8 cm^3.

[32] Radiation Research Corporation, 1150 Shames Drive, Westbury (Long Island), New York.
[33] Applied Physics Corporation, Monrovia, Calif.
[34] M. Kuchnir, Ph.D. thesis, University of Illinois, 1966 (unpublished).
[35] W. R. Abel, A. C. Anderson, and J. C. Wheatley, Rev. Sci. Instr. 35, 444 (1964).
[36] Epibond 100A and Epibond 121 are Epoxy resins distributed by Furane Plastics, Inc., 4516 Brazil Street, Los Angeles 39, Calif.
[37] Manufactured by Buckbee Mears Co., 245 E. 6th Street, St. Paul 1, Minn.
[38] Silver Print, an electrical conducting paint, product of G. C. Electronics Co., Rockford, Ill.

TABLE I. Distances between electrodes as measured at room temperature (cm).

Electrodes	1st cell	2nd cell
Brush–R	0.1	0.1
R–S	0.11	0.00
S–A′	0.11	0.08
A′–A	0.11	0.09
A–B	0.99	1.02
B–B′	0.12	0.11
B′–D	0.09	0.08
D–C	0.07	0.10

In order to improve the uniformity of the field in the drift space, the long ring between A and B had grooves dividing it into 11 cylindrical electrodes at intermediate voltages.

In the second cell the inner walls of the rings were made of gold-plated brass. A lengthwise slot was cut in the inner wall, as in the first cell, to reduce eddy currents, to serve as a sighting hole, and to allow clearance for the leads when sliding the assembly into the case. The drift space had only three cylindrical electrodes, one in contact with grid A, one in contact with grid B, and the central one at the average potential between A and B. These rings were separated by recessed annular disks of 0.013-cm-thick Mylar. The distances between grids and electrodes were measured with a travelling microscope, focusing at different depths in the sighting holes, after the rings were assembled but prior to their introduction into the case. The distances between electrodes as measured at room temperature are presented in Table I. One extra grid, R, was introduced behind the ion source to enhance ion production. In the second cell it was in electrical contact with the source.

With the brush and assembly of rings and grids inside the case, both cells were tested prior to being filled with CMN. The mobility of ions in liquid He^4 was measured at a temperature below the λ point, and the residual magnetism at 4.2 and 2.0°K was measured. After concluding that the cell was operating as expected and that the residual magnetism of the cell would affect the temperature measurements by less than 2.4% at 2.0°K, the powdered CMN was introduced and the cell was sealed by gluing in the end plug with Epibond 121.[36] A leak test was then carried out at room temperature with internal pressures of up to 20 atm. After the cell was installed in the cryostat, but prior to cooling, the electrometer detected currents produced by capacitive coupling between the several electrodes and the collector, and currents carried by ions in the gas-filled cell. It was therefore possible to verify electrical continuity to the electrodes and to test for shorts.

B. Measurements

The measurements were taken in two series of runs, corresponding to the two different cells used. A run usually consisted of an alternating sequence of positive and negative mobility measurements and partial warmup operations as will be described in more detail below. Occasionally, complete scans like Fig. 2 were taken to detect the existence of more than one set of peaks as, for example, might correspond to several charge carriers present with different mobilities. No indication of more than one set of peaks was ever found. At other times, changes in the electric field were made to detect any field dependence of the mobility. No field dependence was ever found for the mobility of negative ions, but some rather strange effects occurred in a limited temperature range for the positive-ion mobility. These effects are what motivated us to repeat the measurements with the second cell, which, as indicated, was changed significantly from the first cell. This is discussed in Sec. III B. The second series of runs was discontinued when a leak developed during the process of increasing the pressure to 29.7 atm.

A typical mobility measurement would start after temperature equilibrium had been established and proceed by (1) resetting the electrode voltages, (2) noting the open-gate and closed-gate currents, (3) recording the initial temperature, (4) plotting the first peak of the frequency-versus-current graph by recording 6–15 points in its neighborhood, (5) again recording the temperature, (6) plotting the next peak at higher frequency and, finally, (7) recording the final temperature. From the current-versus-frequency plots, we obtained ν_1 and ν_2. The value of the mobility was then calculated using Eq. (2). The temperature was taken to be the average temperature during the measuring procedure. If the next point was to be taken at approximately the same temperature but with ions of opposite sign, the batteries were reversed and the procedure was repeated. To obtain the next point at a higher temperature a calculated amount of heat was added to the CrK alum refrigerator by means of an electrical heater. No further experimental data were obtained until the He^3 was again drifting upward in temperature at a rate determined by the residual heat leak.

For the first cell the data were reduced using Eq. (2) with $d=1.10$ cm. A few data obtained from tests carried out on liquid He II prior to the sealing of the cell gave good agreement with the known values of mobility in liquid He II.[1] Similar tests with the second cell with $d=1.11$ cm also gave good agreement in liquid He II in spite of the less uniform field. However, in order to keep the data obtained from both cells within a higher degree of consistency, the second cell was calibrated in relation to the first by imposing the same mobility value on negative ions at 0.1°K and 7.5 atm.

After all measurements in liquid He^3 were taken, the second cell had its bottom plug and CMN removed. It was then transferred to a test cryostat in which the mobility of liquid He^4 was measured. Figure 5 presents

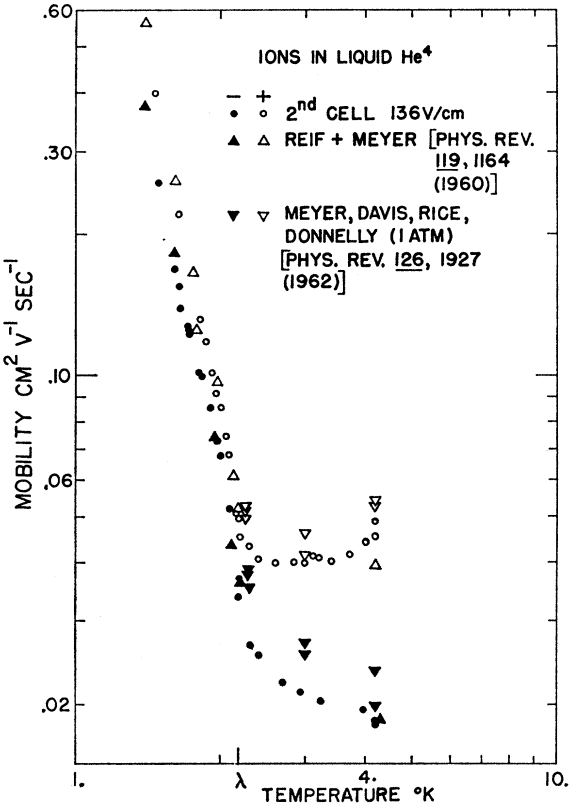

FIG. 5. Ion mobility in liquid He⁴ at low pressures.

these data for comparison with previous work.[1,3] The good agreement gives us added confidence in the calibration procedure used for this cell and in the measurements obtained with the first cell.

III. RESULTS

A. Negative Ions

The mobility data for negative ions are presented in Figs. 6–8. Figure 7 shows the point used to calibrate the second cell, as explained in Sec. II B. Figure 8 also presents the positive-ion mobility at 27.9 atm. It can be seen that the negative-ion mobility is a slowly varying function of temperature. At a given temperature the mobility increases with pressure. The negative-ion data were very reproducible, independent of the electric field or of the cell used. The noticeable scatter in Fig. 6 is mainly due to the slightly different pressures used in the low-pressure runs. Comparing the negative-ion mobility points taken with the second cell in runs 2 and 3, which had the same pressure, a scatter of less than 1% is observed.

The analysis of the systematic errors that might be involved in the quantities that enter Eq. (2) yields a maximum error of $\pm 10\%$ in the absolute value of the negative mobility. A comparison of our data for liquid He⁴ with previous work is shown in Fig. 5 and indicates very good agreement. A more detailed comparison is not meaningful, since differences of up to 30% exist between the previous experiments quoted. The systematic error in the magnetic-temperature scale was smaller than the 3% random error of the temperature measurements.

B. Positive Ions

Figures 9 and 10 present the data obtained for the positive-ion mobility at low pressures and at 7.5 atm, respectively. Unlike the negative-ion mobility, the positive-ion mobility at certain temperatures depended on conditions of the cell prior to the measurement. During measurements with the first cell we were not completely

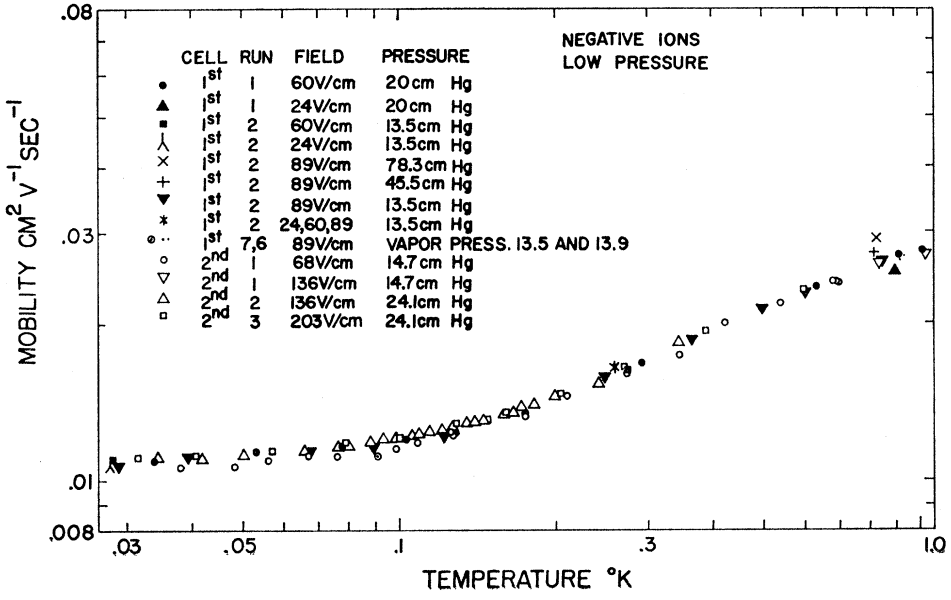

FIG. 6. Mobility of negative ions in liquid He³ at low pressures.

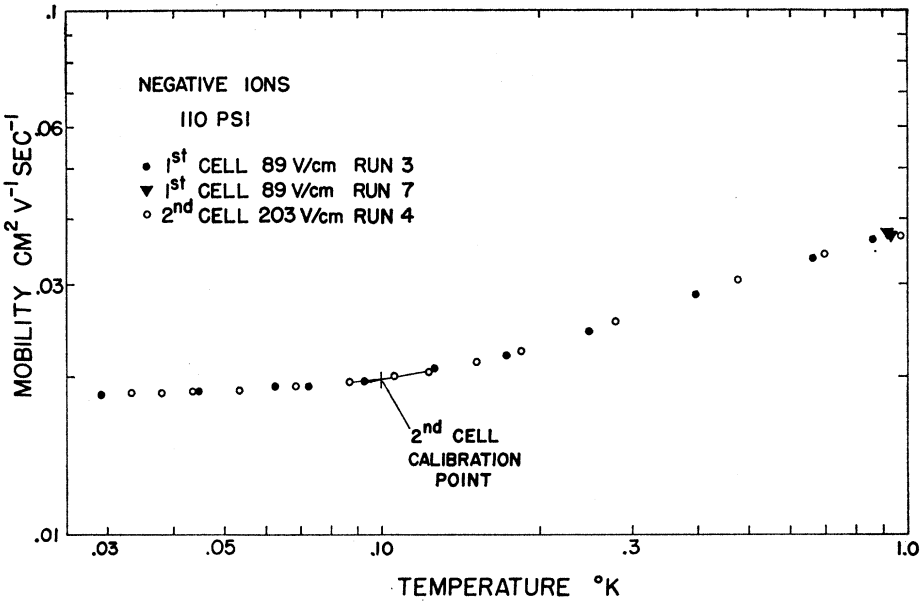

FIG. 7. Mobility of negative ions in liquid He³ at 7.5 atm.

aware of this effect, but we suspected its existence from a rather sharp drop of the positive-ion mobility between the values of 0.11 and 0.045 cm²/V sec as the temperature increased from 0.065 to 0.3°K. It was not known whether the result was instrumental or not. In the event that it was connected with some space charge formation associated with the imperfect conductivity of the silver-painted cell wall, the second cell was designed with gold-plated brass walls and a different electrode arrangement along the walls as was explained above. A more careful investigation of the positive-ion mobility made with the second cell at low pressures revealed the following. Above 0.065°K the mobility decreased slowly with time as did the open gate current i_0. It became clear in run 1 of the second cell that the sharp drop observed in the mobility was due in part to long delays before taking the measurements, during which the cell was left polarized for positive ions. It was realized, in retrospect, that the data from the first cell were consistent with this time and polarization dependence.

Having the above effect in mind, the mobility measurements in runs 2–4 of the second cell were taken immediately after a period during which the cell was negatively polarized. For run 2, heat was added to the refrigerator in relatively small amounts (10^4 erg), and a continuous dependence on temperature was obtained up to 0.15°K. At this temperature a larger amount of heat (2×10^5 erg) was added and a discontinuous drop of 20%

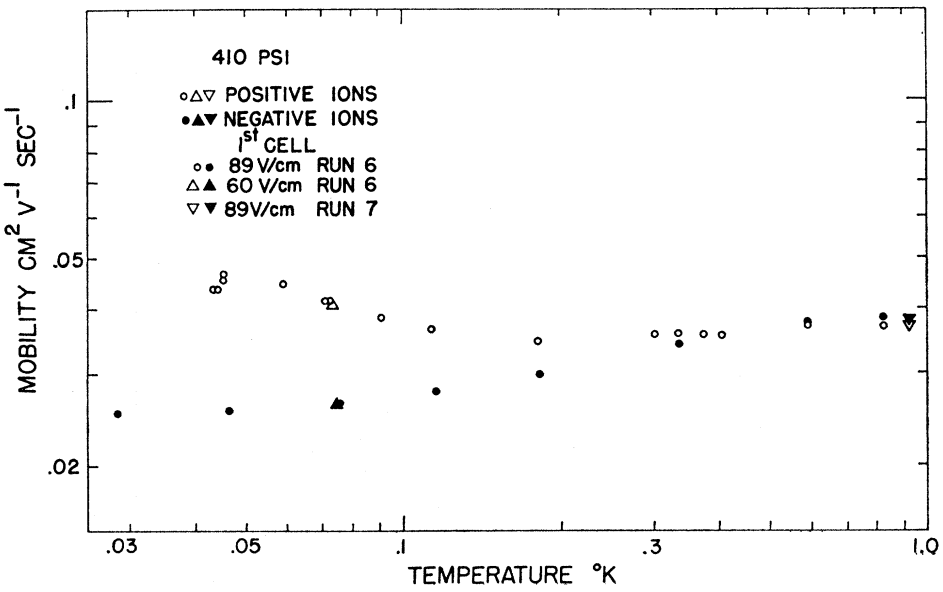

FIG. 8. Ion mobility in liquid He³ at 27.9 atm.

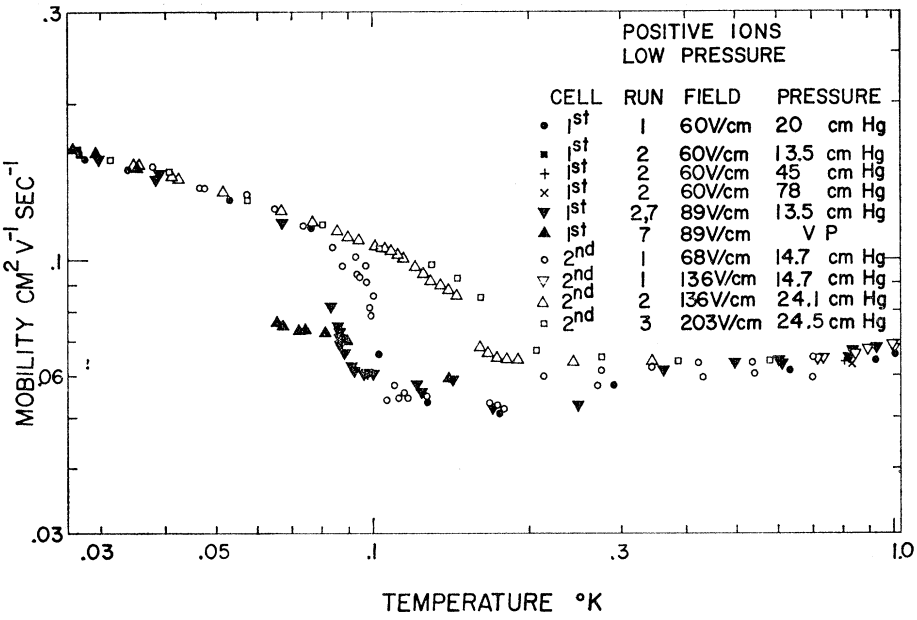

FIG. 9. Mobility of positive ions in liquid He^3 at low pressures.

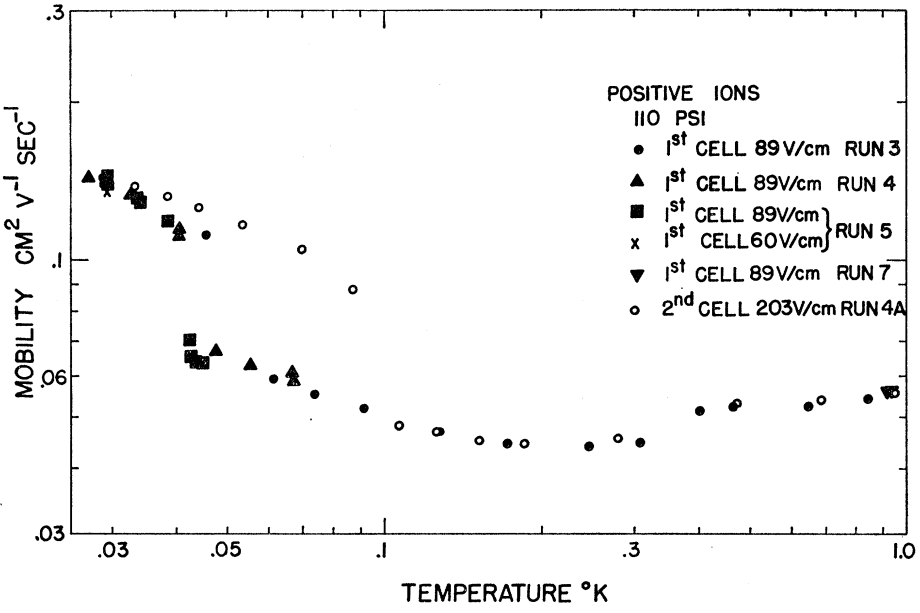

FIG. 10. Mobility of positive ions in liquid He^3 at 7.5 atm.

in the positive mobility was noticed. This fact could suggest that the effect of convection may also play a role for those positive-ion mobilities which were irreproducible. In this same region a dependence of the mobility on the electric field was also observed from runs 2 and 3 with the second cell. The above effects apparently did not exist for temperatures below roughly 0.06°K at low pressure or below 0.03°K at 7.5 atm. At temperatures above 0.3°K the effects do exist but are smaller (~7%), as points of run 1 with the second cell indicate.

With the presently available data it seems likely that the irreproducibilities observed in the positive-ion mobilities are experimentally based. They do present some of the features that L. Meyer[39] and G. Careri[40] attributed to impurities in colloidal suspension. Note also that the He^4 content of our He^3 was of order 1 in 10^4. Assuming that the effects were caused by impurities, the positive-mobility measurements taken in runs 2–4 with the second cell were preceded by an electrolitical cleaning of the cell with negative ions, and can be considered of higher reliability. In addition, it would appear that no

[39] Lothar Meyer, Phys. Rev. 148, 145 (1966).
[40] G. Careri (private communication).

TABLE II. Ion-structure parameters and approximation limits.

Pressure (atm)	ϵ_F/k[a] (°K)	R_-[b] (Å)	M_-[c] (M_{He^3})	$m\epsilon_F/M_-k$ (°K)	R_+[d] (Å)	M_+[e] (M_{He^3})	$m\epsilon_F/M_+k$ (°K)
0.26	1.7	23	390	0.012	6.1	40	0.12
7.5	1.3	16	160	0.034	6.6	50	0.10
27.9	1.1	12	94	0.066	10	130	0.045

[a] $\epsilon_F/k=[\hbar^2/(2mk)](3\pi^2N_0/V_0)^{2/3}$, where m is the Fermion effective mass (Ref. 44), N_0 is Avogadro's number, and V_0 is the He³ molar volume (Ref. 45).
[b] R_-, the radius of the negative ion, was determined using Eq. (4) with γ taken from Ref. 46.
[c] M_-, the mass of the negative ion, was taken as the hydrodynamical correction $\frac{1}{2}(\frac{4}{3}\pi R^3\rho)$, where ρ is the liquid density.
[d] R_+ was computed according to Atkins model (Refs. 6 and 7) using the molar-volume data of Ref. 45 and the melting pressure of Ref. 47 at $T=0.04$°K.
[e] M_+ was taken as the mass of the solid cluster plus its hydrodynamical correction.

electrolitical cleaning is achieved with positive ions, but rather an impurity buildup seems to be observed. Nevertheless, it is remarkable that the mobility tends to be either high or low, almost as if there were two branches to the curve.

In spite of the effects just discussed it may be concluded that the positive-ion mobility decreases with increasing pressure and is larger than the negative mobility except above 0.5°K at 27.9 atm.

C. General Features

Comparing our mobility data in liquid He³ with existing mobility data in liquid He⁴ we notice the following:

(1) The mobility in liquid He³ is much lower than in liquid He⁴, a factor of 10^4 at 0.6°K.

(2) The temperature dependences are quite different, being much weaker in the case of He³.

(3) The positive-ion mobility decreases with pressure in both liquid He³ and liquid He⁴. The negative-ion mobility in liquid He⁴ is known to increase with pressures up to 2.6 atm and then decrease with further pressure increase. Our data, however, suggest that in liquid He³ the negative-ion mobility increases with pressure monotonically, although this cannot be uniquely determined from measurements at only three pressures.

IV. DISCUSSION

The available data on the mobility of ions in liquid He³ prior to this work[3–5] have been analyzed mainly according to the simple model of a sphere moving without slippage in a fluid and obeying Stokes's Law. In this picture a relation between the mobility μ, the radius of the sphere R, and the viscosity η can be established and is known as Walden's Rule:

$$\mu\eta=(e/4\pi)R^{-1},$$

where e is the ionic charge. Using our mobility data at low pressure and the viscosity given by Betts *et al.*,[41] this model predicts a shrinking of the ions as the temperature is lowered. More quantitatively, at 1°K and 0.26 atm the positive-ion radius is ~4 Å and the negative ~10 Å; they shrink to ~1.5 Å at 0.15 and 0.05°K, respectively. It is obvious that this classical model does not hold for temperatures below 1°K if the sphere is to have a temperature-independent radius, and has no meaning for a radius smaller than 3 Å since the radius of a He³ atom is ~1.3 Å.[42]

The mobility, from the point of view of statistical mechanics, is treated by considering the interaction between the ions and a dense gas representing the liquid He³. At high temperatures this gas would be a Boltzmann gas and the mobility would be expected to have a $T^{-1/2}$ temperature dependence.[43] At very low temperatures the gas would be a degenerate Fermi system and the mobility would be expected to have a temperature dependence of T^{-2} as derived independently by Abe and Aizu[24] and by Clark.[25] For intermediate temperatures, Davis and Dagonnier[26] have derived the expression

$$\mu=\frac{3\pi}{8m^2\sigma}\frac{e\hbar^3}{(\epsilon_F^2+\frac{1}{3}\pi^2k^2T^2)}, \tag{3}$$

which assumes the momentum of the ion to be very large compared to the Fermi momentum. In this expression, σ is the collision cross section, ϵ_F is the Fermi energy, m is the effective mass of the Fermions, $2\pi\hbar$ is Plank's constant, and k is Boltzmann's constant.

Because of the assumptions used in the above treatments, the $T^{-1/2}$ dependence is expected for $T\gg\epsilon_F/k$, the $(\epsilon_F^2+\frac{1}{3}\pi^2k^2T^2)^{-1}$ dependence for $m\epsilon_F/Mk\ll T\ll\epsilon_F/k$, and the T^{-2} dependence for $T\ll m\epsilon_F/Mk$. In order to compare the experimental data with the above predictions the effective mass M and cross section of the ions should be determined by independent experiments. In the absence of such data for liquid He³ we use the cluster model and the simple bubble model to estimate the above temperature limits. The results are presented in Table II.[44–47] It will be noted that, with respect to the temperature dependence, the existing theories do not

[41] D. S. Betts, D. W. Osborne, B. Welber, and J. Wilks, Phil. Mag. 8, 977 (1963).

[42] T. F. O'Malley, Phys. Rev. **130**, 1020 (1963).

[43] E. H. Kennard, *Kinetic Theory of Gases* (McGraw-Hill Book Co., New York, 1938), p. 466.

[44] J. C. Wheatley, *Quantum Fluids*, edited by D. F. Brewer (John Wiley & Sons, Inc., New York, 1966), p. 183.

[45] E. R. Grilly and R. L. Mills, Ann. Phys. (N. Y.) **8**, 1 (1959); C. Boghosian, H. Meyer, and J. E. Rives, Phys. Rev. **146**, 110 (1966).

[46] N. Bernardes and D. F. Brewer, Rev. Mod. Phys. **34**, 190 (1962).

[47] A. C. Anderson, W. Reese, and J. C. Wheatley, Phys. Rev. **130**, 1644 (1963).

TABLE III. Pressure dependence of negative mobility at 0.03°K.

Pressure (atm)	$(\mu_-)_{DD}$ [Eq. (3)] (cm²/V sec)	μ_- Expt (cm²/V sec)	$(\mu_-)_{DD}/\mu_-$
0.26	0.35	0.011	32
7.5	0.57	0.019	31
27.9	0.73	0.025	29

explain the data except for a qualitative agreement found between our low-temperature negative-ion data and Davis and Dagonnier's theory. The low-temperature T^{-2} dependence may yet be valid, but for temperatures below the ones attained with this experiment.

In the temperature-independent region observed for negative ions we can compare the observed pressure dependence with that predicted by Eq. (3). Let us take for the negative ion a simple bubble model assuming the electron to be a particle in a box, and assuming the surface tension of the liquid to be independent of pressure. The total energy ϵ_t involved in the formation of the bubble is

$$\epsilon_t=\pi^2\hbar^2/2m_eR^2+\tfrac{4}{3}\pi pR^3+4\pi R^2\gamma,$$

where the right side is the sum of the electron's zero-point energy, the work done against the pressure p, and the work done against the surface tension γ, respectively. Minimizing ϵ_t with respect to the radius R of the bubble, we have

$$\frac{d\epsilon_t}{dR}=0=-\frac{\pi^2\hbar^2}{m_eR^3}+4\pi pR^2+8\pi R\gamma. \tag{4}$$

We now have an expression from which R can be determined graphically. Using $\sigma=\pi R^2$ in Eq. (3) we get the values shown in Table III, where we see an agreement on the pressure dependence of the mobility to within 10%, although the absolute value of the measured mobility is too small by one order of magnitude. In addition, the weak temperature dependence found in Eq. (3) is opposite to that observed experimentally.

In conclusion, it is not clear if the Fermi behavior of liquid He^3 has manifested itself in the ion mobility at temperatures down to 0.03°K. It would therefore be useful to extend the measurements to still lower temperatures. It would also be of considerable importance to measure the ion mobilities in dilute solutions of He^3 in liquid He^4 at low temperatures, since the He^3 can here be represented as a weakly interacting Fermi gas and the ion parameters in liquid He^4 have been measured independently. Unfortunately, our own interest in the dilute solutions came after the conclusion of the measurements discussed in this paper.

Errata

Auto-ionizing States in the Alkali Atoms with Microsecond Lifetimes, P. FELDMAN AND R. NOVICK [Phys. Rev. **160**, 143 (1967)]. Page 153, caption for Fig. 8: Instead of "Excitation function for metastable auto-ionizing states in potassium," it should read "Excitation function for metastable auto-ionizing states in rubidium." Page 154, caption for Fig. 9: Instead of "Excitation function for metastable auto-ionizing states in rubidium," it should read "Excitation function for metastable auto-ionizing states in potassium."

Approach to the Bound-State Three-Body Problem with Application to the Helium-Like Atom, J. R. JASPERSE AND M. H. FRIEDMAN [Phys. Rev. **159**, 69 (1967)]. In addition to solutions of the form given by Eq. (12), Sec. III, there will also be solutions of the form

$$\Psi^{S,A}=\psi_{12}{}^{o,e}(\mathbf{r}_{12},\boldsymbol{\varrho}_3)-\psi_{12}{}^{o,e}(\mathbf{r}_{23},\boldsymbol{\varrho}_1)+\psi_{31}{}^{e,o}(\mathbf{r}_{31},\boldsymbol{\varrho}_2).$$

The analysis for these states is the same as for those treated explicitly in the paper.